# Robust Quasi NID Current and Flux Control of an Induction Motor for Position Control

Marc van Duijnhoven *
Eindhoven Technical University
Department of Electrical Engineering
5600 MB Eindhoven

Marian J. Błachuta †
Silesian Technical University
Department of Automatic Control
16 Akademicka St., PL 44-101, Gliwice, Poland

**Abstract**

In the paper, a new control design method called Dynamic Contraction method is applied to the flux and quadrature current robust control of an induction motor operated using the field orientation principle. The resulting input-output decoupled and linearized drive is then used for time-optimal position control. Two control structures providing a practically time-optimal control are presented and compared.

## 1 Introduction

The last 25 years there was a fast development of new power semi-conductors and digital electronics. Due to the availability of these new devices and the price decrease a great deal of research has been done in the field of controlling AC-drives.
The induction motor is indispensable because of its ruggedness and low cost but until recently its control applications were restricted by the difficulties in controlling its torque and speed.
The great step towards induction motor control was invention of the field orientation control principle (Blaschke, 1971) which allows to eliminate the coupling between two control inputs provided that the flux is stabilized.
It is usually assumed that position and the drive currents are measured, and flux, flux-angle, speed and torque are observed. The parameters, especially the rotor resistance, vary significantly from their nominal values. Therefore controllers should be robust against these effects. The position control problem is split in two different parts as shown in Fig. 1 and the paper concentrates mainly on inner loops.
With increasing rated power the electromagnetic transients become slower and slower, and to arrive at good overall performance for middle range rated power motors ($>$1kW) they should be accelerated by control systems. In contrast to micro-motors high gains in control loops and large magnitudes of control signals are then required, which is not always possible. This is the problem dealt with in this paper.

*E-mail: *marcd@stack.nl*.
†E-mail: *blachuta@ia.gliwice.edu.pl.* The support from the Polish Committee for Scientific Research (KBN) and a fellowship granted by the MED'99 Organizing Committee are appreciated.

Several approaches have been applied in literature: sliding mode control (Bartolini, Pisu, Marchesoni, and Usai, 1998), adaptive nonlinear control (Marino, Peresada, and Valigi, 1993), and PI linearizing control (Bodson, Chiasson, and Novotnak, 1994). Recently, a new nonlinear control method called Dynamic Contraction Method (DCM) was developed (Yurkevich, 1995a,b). This method offers performance similar to that of Nonlinear Inverted Dynamics (NID) but it works well for uncertain nonlinear systems. In the paper the DCM method will be applied to the AC-motor in field coordinates to linearize and decouple the flux and the current channels.

The paper is organized as follows. In section 2 and 3 the AC-motor model and field oriented control are introduced. In section 4 the DCM method is introduced, and applied to the induction motor in section 5. In section 6 the inner loops are thorougly analyzed. In section 7 a time optimal control is designed (the outer loops), and the paper is concluded with remarks that additionaly base on the research done by van Duijnhoven (1998)

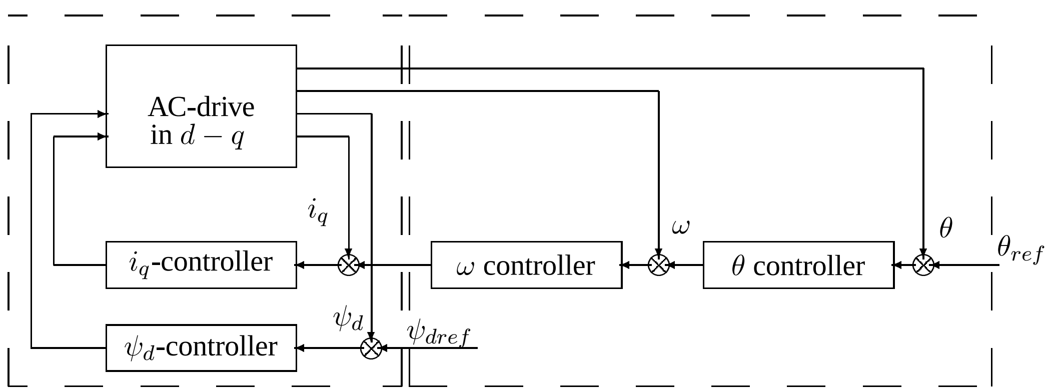


Figure 1: AC-motor position control in field coordinates

## 2 Induction Motor

The dynamics of a 2-phase induction motor are described in $a-b$ coordinates by the following 6th order model:

$$\begin{aligned}
\frac{d\theta}{dt} &= \omega && (1)\\
\frac{d\omega}{dt} &= \mu(\psi_{ra}i_{sb} - \psi_{rb}i_{sa}) - \frac{T_L}{J} && (2)\\
\frac{d\psi_{ra}}{dt} &= -\eta\psi_{ra} - n_p\omega\psi_{rb} + \eta M i_{sa} && (3)\\
\frac{d\psi_{rb}}{dt} &= -\eta\psi_{rb} + n_p\omega\psi_{ra} + \eta M i_{sb} && (4)\\
\frac{di_{sa}}{dt} &= \eta\beta\psi_{ra} + \beta n_p\omega\psi_{rb} - \gamma i_{sa} + \frac{1}{\sigma L_s}u_{sa} && (5)\\
\frac{di_{sb}}{dt} &= -\beta n_p\omega\psi_{ra} + \eta\beta\psi_{rb} - \gamma i_{sb} + \frac{1}{\sigma L_s}u_{sb}, && (6)
\end{aligned}$$

with

$$\sigma = 1 - \frac{M^2}{L_sL_r}, \eta = \frac{R_r}{L_r}, \beta = \frac{M}{\sigma L_sL_r}, \mu = \frac{n_pM}{JL_r}, \gamma = \frac{M^2R_r}{\sigma L_r^2L_s} + \frac{R_s}{\sigma L_s} \quad (7)$$

The induction motor usually consists of three stator windings and three rotor windings. As shown by Krause and Thomas (1965) the above equations can be seen as a two phase equivalent representation of a 3-phase system. This model may also be used for squirrel cage rotors.

# 3 Field oriented control

The idea of field oriented control introduced by Blaschke (1971) consists in rewriting the dynamic equations of the induction motor in a reference frame that rotates with the rotor flux vector. Denoting its angular position by $\rho$, one gets

$$\rho(t) = \arctan \frac{\psi_b(t)}{\psi_a(t)} \tag{8}$$

The transformation of currents, fluxes and voltages to two components which are perpendicular and parallel to the field is referred to as the direct-quadrature or DQ transformation.
We have:

$$\begin{pmatrix} i_d \\ i_q \end{pmatrix} = \begin{bmatrix} \cos\rho & \sin\rho \\ -\sin\rho & \cos\rho \end{bmatrix} \begin{pmatrix} i_a \\ i_b \end{pmatrix}, \ \begin{pmatrix} \psi_d \\ \psi_q \end{pmatrix} = \begin{bmatrix} \cos\rho & \sin\rho \\ -\sin\rho & \cos\rho \end{bmatrix} \begin{pmatrix} \psi_a \\ \psi_b \end{pmatrix}, \tag{9}$$

so that

$$\begin{aligned} \psi_d &= \sqrt{\psi_a^2 + \psi_b^2} = |\psi| \\ \psi_q &= 0 \end{aligned} \tag{10}$$

In the field coordinates the induction motor is described by the following system of equations:

$$\frac{d\omega}{dt} = \mu\psi_d i_q - T_L/J \tag{11}$$

$$\frac{d\psi_d}{dt} = -\eta\psi_d + \eta M i_d \tag{12}$$

$$\frac{di_d}{dt} = -\gamma i_d + \eta\beta\psi_d + n_p\omega i_q + \eta M \frac{i_q^2}{\psi_d} + \frac{1}{\sigma L_s} u_d \tag{13}$$

$$\frac{di_q}{dt} = -\gamma i_q - \beta n_p \omega\psi_d - n_p\omega i_d - \eta M \frac{i_q i_d}{\psi_d} + \frac{1}{\sigma L_s} u_q \tag{14}$$

$$\frac{d\rho}{dt} = n_p\omega + \eta M \frac{i_q}{\psi_d} \tag{15}$$

The inverse transformation, IDQ, applied to voltages

$$\begin{pmatrix} u_a \\ u_b \end{pmatrix} = \begin{bmatrix} \cos\rho & -\sin\rho \\ \sin\rho & \cos\rho \end{bmatrix} \begin{pmatrix} u_d \\ u_q \end{pmatrix} \tag{16}$$

shows that in the steady-state when both $u_d$ and $u_q$ are constant and $\dot{\rho}(t) = \omega_0$ then the supplying voltages $u_a$ and $u_b$ become sinusoidal, $u_a(t) = u_a^m \sin(\omega_o t + \phi)$, $u_a(t) = u_b^m \cos(\omega_o t + \phi)$, and they are more complicated functions of time in transient states. It is assumed here that the AC-drive is fed by a voltage source inverter working at frequencies high enough for a good dynamic performance and smooth operation at stillstand.

# 4 Nonlinear Control - Dynamic Contraction Method

## 4.1 Preliminaries

Let us consider a nonlinear time-varying system in the following form:

$$\dot{\boldsymbol{x}} = \boldsymbol{f}(t,\boldsymbol{x}) + \boldsymbol{B}(t,\boldsymbol{x})\boldsymbol{u}(t), \qquad \boldsymbol{x}(0) = \boldsymbol{x}_0 \tag{17}$$

$$\boldsymbol{y} = \boldsymbol{g}(t,\boldsymbol{x}) \tag{18}$$

where $\boldsymbol{x}(t)$ is an $n$-dimensional state vector, $\boldsymbol{y}(t)$ is a $p$-dimensional output vector and $\boldsymbol{u}(t)$ is a $p$-dimensional control vector.
Following Yurkevich (1995a), assume that each output $y_i$ can be differentiated $\alpha_i$ times until the control input appears. This results in the following equation:

$$\boldsymbol{y}^* = \boldsymbol{c}^*(t,\boldsymbol{x}(t)) + \boldsymbol{B}^*(t,\boldsymbol{x})\boldsymbol{u}, \qquad \boldsymbol{x}(0) = \boldsymbol{x}_0, \tag{19}$$

where

$$\boldsymbol{y}^* = \left[y_1^{(\alpha_1)}, y_2^{(\alpha_1)}, \ldots, y_p^{(\alpha_p)}\right]'. \tag{20}$$

Assume that a reference model for transients of $y_i^{(\alpha_i)}(t)$ is given in the following vector differential equation:

$$y_i^{(\alpha_i)}(t) = F_i(\boldsymbol{y}_i(t), \boldsymbol{r}_i(t)), i = 1, 2 \ldots p \tag{21}$$

where $F_i$ is referred to as the desired dynamics of $y_i(t)$, and

$$\boldsymbol{y}_i = [y_i, y_i^{(1)}, \ldots, y_i^{(\alpha_i - 1)}]',\ \boldsymbol{r}_i = [r_i, r_i^{(1)}, \ldots, r_i^{(\alpha_i - 1)}]'. \tag{22}$$

In case the components $y_i^{(\alpha_i)}$ are independent and the control inputs $u_i$ are decoupled the $i$th element of $\boldsymbol{y}^*$ could be written as:

$$y_i^{(\alpha_i)} = -\sum_{j=0}^{\alpha_i - 1} a_{i,j} y_i^{(j)} + \sum_{j=0}^{\alpha_i - 1} b_{i,j} r_i^{(j)} \tag{23}$$

The difference between the desired and the actual response of the system is defined as:

$$\boldsymbol{\Delta} = \boldsymbol{F}(\boldsymbol{y}(t), \boldsymbol{r}(t)) - \boldsymbol{y}^*(t) \tag{24}$$

The control system to be designed must be stable and provide the following condition:

$$\boldsymbol{\Delta}(t, \boldsymbol{x}(t), \boldsymbol{u}(t)) = 0 \tag{25}$$

Equation (25) can be solved with respect to $\boldsymbol{u}(t)$ analitically leading to NID control algorithm $\boldsymbol{u}^{nid}(t)$:

$$\boldsymbol{u}^{nid}(t) = \boldsymbol{B}^*(t,\boldsymbol{x})^{-1}[\boldsymbol{F}(\boldsymbol{y}(t), \boldsymbol{r}(t)) - \boldsymbol{c}^*(t, \boldsymbol{x}(t))] \tag{26}$$

This control law may be used only if there is complete information about disturbances, model parameters and the state of the system. Therefore it has no real practical value.

## 4.2 The Dynamic Contraction Method (DCM)

Let us introduce nonsingular matrices $\boldsymbol{K}_0$, and $\boldsymbol{K}_1$ whose meaning will be discussed later. $\boldsymbol{K}_1$ is usually a diagonal matrix. In the next equation the new control input $\boldsymbol{v}$ is defined as:

$$\boldsymbol{u}(t) = \boldsymbol{K}_0\boldsymbol{K}_1\boldsymbol{v}(t) \tag{27}$$

The following equation was discussed by Yurkevich (1995a):

$$\sum_{j=0}^{q} \boldsymbol{\mu}^j \boldsymbol{D}_j \boldsymbol{v}^{(j)} = k\boldsymbol{\Delta}, \qquad \vec{\boldsymbol{v}}(0) = \vec{\boldsymbol{v}}_0, \tag{28}$$

with $\boldsymbol{\mu} =$ diag $\{\mu_1, \mu_2, \ldots, \mu_p\}$ and $q \geq \max \alpha_i$. Here $\mu_i$ are small positive parameters, and $\boldsymbol{D}_{q-1}, \ldots, \boldsymbol{D}_0$ are diagonal matrices and $\vec{\boldsymbol{v}}(t) = \left[\boldsymbol{v}', \boldsymbol{v}^{(1)\prime}, \ldots, \boldsymbol{v}^{(q-1)\prime}\right]'$. Using Eqs. (23), (24) and (27) the following controller equation can be written for each $i$-th channel:

$$\sum_{j=0}^{q_i} \mu_i^j d_{i,j} v_i^{(j)} = k_i(\sum_{j=0}^{\alpha_i-1} b_{i,j} r_i^{(j)} - \sum_{j=0}^{\alpha_i-1} a_{i,j} y_i^{(j)}), \qquad \boldsymbol{v_i}(0) = \boldsymbol{v}_{i,0}, \tag{29}$$

where $\boldsymbol{v_i} = \left[v_i, v_i^{(1)}, \ldots, v_i^{(q_i-1)}\right]'$. Since $q_i \geq \alpha_i$ the controller is proper and realizable without differentiation.

Assuming that $\boldsymbol{v}(t)$ changes much faster then $\boldsymbol{x}(t), \boldsymbol{y}(t)$, and $\boldsymbol{r}(t)$ our control problem can be translated into a two time scale problem. One for the fast motions (the control) and one for the slow motions (the states). The new fast time scale is defined as $\tau = \mu^{-1}t$, where $\mu = \max(\mu_i)$ is a small positive parameter.

### 4.2.1 Fast motions

From equations (17), (19), (24), (27), (28) the close loop system can be rewritten as:

$$\dot{\boldsymbol{x}} = \boldsymbol{f}(t, \boldsymbol{x}) + \boldsymbol{B}(t, \boldsymbol{x})\boldsymbol{K}_0\boldsymbol{K}_1\boldsymbol{v}, \qquad \boldsymbol{x}(0) = \boldsymbol{x}_0 \tag{30}$$

$$\boldsymbol{\Gamma}\boldsymbol{v} + \sum_{i=1}^{q} \boldsymbol{\mu}^i \boldsymbol{D}_i \boldsymbol{v}^{(i)} = k\left[\boldsymbol{F} - \boldsymbol{c}^*(t, \boldsymbol{x})\right], \qquad \vec{\boldsymbol{v}}(0) = \vec{\boldsymbol{v}}_0, \tag{31}$$

where $\boldsymbol{\Gamma}$ is defined as:

$$\boldsymbol{\Gamma} = \boldsymbol{D}_0 + k\boldsymbol{B}(t, \boldsymbol{x})\boldsymbol{K}_0\boldsymbol{K}_1, \qquad \boldsymbol{K}_1 = \text{ diag}\,\{k_1, \ldots, k_p\} \tag{32}$$

Taking lim $\mu \to 0$ and returning to the primary time scale with $t = \mu\tau$ we obtain the fast motion system which is defined by:

$$\boldsymbol{\Gamma}\boldsymbol{v} + \sum_{i=1}^{q} \boldsymbol{\mu}^i \boldsymbol{D}_i \boldsymbol{v}^{(i)} = k\left[\boldsymbol{F} - \boldsymbol{c}^*\right], \qquad \vec{\boldsymbol{v}}(0) = \vec{\boldsymbol{v}}_0, \tag{33}$$

where $\boldsymbol{F}$ and $\boldsymbol{c}^*$ are assumed constant if there is good time separation between the fast and the slow motions. The matrix $\boldsymbol{K}_0$ is often chosen as $(\boldsymbol{B}^*)^{-1}$ to decouple the fast motion subsystem and thus to simplify the design. Matrix $\boldsymbol{K}_1$ can be used to tune the control inputs.

#### 4.2.2 Slow motions

The slow motion system is found by using equations (19), (27), (35) and taking $\mu \to 0$.

$$\boldsymbol{y}^* = \boldsymbol{F} + k^{-1}\boldsymbol{D_0}\left[k^{-1}\boldsymbol{D_0} + \boldsymbol{B}^*(t,\boldsymbol{x})\boldsymbol{K}_0\boldsymbol{K}_1\right]^{-1}[\boldsymbol{c}^*(t,\boldsymbol{x}) - \boldsymbol{F}] \tag{34}$$

The steady state of the fast motion time system is defined by:

$$\boldsymbol{v}^s = k\boldsymbol{\Gamma}^{-1}[\boldsymbol{F} - \boldsymbol{c}^*] \tag{35}$$

Using $\boldsymbol{u}^{nid} = \boldsymbol{K}_0\boldsymbol{K}_1\boldsymbol{v}^{nid}(t)$ this can be rewritten into the following form:

$$\boldsymbol{v}^s = \boldsymbol{v}^{nid} + \boldsymbol{\Gamma}^{-1}\boldsymbol{D_0}[\boldsymbol{B}^*\boldsymbol{K}_0\boldsymbol{K}_1]^{-1}[\boldsymbol{c}^*(t,\boldsymbol{x}) - \boldsymbol{F}] \tag{36}$$

If $\boldsymbol{D}_0 = 0$ or $\boldsymbol{D}_0 \neq 0$ but $k \to \infty$ then $\boldsymbol{v}^s \to \boldsymbol{v}^{nid}$ and $\boldsymbol{y}^* \to \boldsymbol{F}$. As a result, the DCM control will converge to the NID solution.
However, in contrast to NID, the DCM method can be used in systems with incomplete information about $\boldsymbol{f}(t,\boldsymbol{x})$, $\boldsymbol{g}(t,\boldsymbol{x})$ and $\boldsymbol{B}(t,\boldsymbol{x})$ and varying parameters.

## 5 Applying DCM to the Induction Motor Control

The goal of this section is to apply the DCM method to our MIMO motor system, and design a current and flux controller. Rewriting the motor equations (11) in state space gives:

$$\dot{\boldsymbol{x}} = \begin{bmatrix} \mu x_2 x_4 - T_L/J \\ -\eta x_2 + \eta M x_3 \\ -\gamma x_3 + \eta\beta x_2 + n_p x_1 x_4 + \eta M x_4^2/x_2 \\ -\gamma x_4 - \beta n_p x_1 x_2 - n_p x_1 x_3 - \eta M x_3 x_4/x_2 \\ n_p x_1 + \eta M x_4/x_2 \end{bmatrix} + \begin{bmatrix} 0 & 0 \\ 0 & 0 \\ \frac{1}{\sigma L_s} & 0 \\ 0 & \frac{1}{\sigma L_s} \\ 0 & 0 \end{bmatrix}\boldsymbol{u}, \tag{37}$$

with $x_1 = \omega$, $x_2 = \psi_d$, $x_3 = i_d$, $x_4 = i_q$, $x_5 = \rho$, $u_1 = u_d$, and $u_2 = u_q$.
Let us denote $y_1 = i_q$, $y_2 = \psi_d$ and $\boldsymbol{y}^* = [y_1^{(1)}, y_2^{(2)}]'$. Then we have

$$\boldsymbol{y}^* = \boldsymbol{c}^*(t,\boldsymbol{x}) + \boldsymbol{B}^*\boldsymbol{u}, \tag{38}$$

with

$$\begin{aligned} \boldsymbol{c}^*(t,\boldsymbol{x}) &= \begin{bmatrix} -\gamma x_4 - \beta n_p x_1 x_2 - n_p x_1 x_3 - \eta M x_3 x_4/x_2 \\ \eta M(-\gamma x_3 + \eta\beta x_2 + n_p x_1 x_4 + \eta M x_4^2/x_2) \end{bmatrix} \\ \boldsymbol{B}^* &= \begin{bmatrix} 0 & 1/(\sigma L_s) \\ \eta M/(\sigma L_s) & 0 \end{bmatrix}. \end{aligned} \tag{39}$$

$\boldsymbol{B}^*$ is diagonal and does not depend on $x$ and unknown parameters, which greatly simplifies the analysis and design of the control system.

### 5.1 Controllers

Since the relative order of the quadrature current $y_1 = i_q$ is equal to 1 and the relative order of the flux $y_2 = \psi_d$ is equal to 2, the controller equations can be expressed in terms of time constants and damping coefficients as follows:

$$\mu_q v_q^{(1)} + d_{0,q} v_q = k_1[-i_q^{(1)} + \tau_q^{-1}(i_{qref} - i_q)] \tag{40}$$

$$\mu_d^2 v_d^{(2)} + 2d_{1,d}\mu_d v_d^{(1)} + d_{0,d} v_d = k_2[-\psi_d^{(2)} + \tau_d^{-2}(\psi_{dref} - 2\alpha_d\tau_d\psi_d^{(1)} - \psi_d)] \tag{41}$$

or in a slightly modified form:

$$\begin{aligned} \mu_q v_q^{(1)} + d_{0,q} v_q &= k_q[-\tau_q i_q^{(1)} - i_q + i_{qref}] \quad (42) \\ \mu_d^2 v_d^{(2)} + 2d_{1,d}\mu_d v_d^{(1)} + d_{0,d} v_d &= k_d[-\tau_d^2 \psi_d^{(2)} - 2\alpha_d \tau_d \psi_d^{(1)} - \psi_d + \psi_{dref}] \quad (43) \end{aligned}$$

The controllers in (40)-(41) can also be presented in the transfer function forms:

$$v_q(s) = k_q \left[ \frac{1}{\mu_q s + d_{0,q}} i_{qref}(s) - \frac{(1+\tau_q s)}{\mu_q s + d_{0,q}} i_q(s) \right] \quad (44)$$

$$v_d(s) = k_d \left[ \frac{1}{\mu_d^2 s^2 + 2d_{1,d}\mu_d s + d_{0,d}} \psi_{dref}(s) - \frac{\tau_d^2 s^2 + 2\alpha_d \tau_d s + 1}{\mu_d^2 s^2 + 2d_{1,d}\mu_d s + d_{0,d}} \psi_d(s) \right] \quad (45)$$

Putting $d_{0,q} = 0$ and $d_{0,d} = 0$ introduces the integral action to the above controllers.

## 5.2 Controllers design rules

Using $k = 1$, and $\boldsymbol{K}_0 = (\boldsymbol{B}^*)^{-1}$, then the fast motions equation takes the following form:

$$\boldsymbol{\mu}^2 \boldsymbol{D}_2 \boldsymbol{v}^{(2)} + \boldsymbol{\mu} \boldsymbol{D}_1 \boldsymbol{v}^{(1)} + \boldsymbol{\Gamma} = k\left[\boldsymbol{F} - \boldsymbol{c}^*\right], \quad (46)$$

$$\boldsymbol{\Gamma} = \boldsymbol{D_0} + \boldsymbol{K}_1 \quad (47)$$

for the motor control. The parameters that determine the fast dynamics of the controller can now be chosen.

**The current controller:** The characteristic equation for the current controller can be written as:

$$\frac{\mu_q}{d_{0,q} + k_q} s + 1 = 0 \quad (48)$$

Denoting

$$\mu_q^0 = \frac{\mu_q}{d_{0,q} + k_q}, \quad (49)$$

then the design rule to have a good time scale separation is:

$$\mu_q^0 \leq 0.1\tau_i \quad (50)$$

**The flux controller:** The characteristic equation for the flux controller is:

$$\frac{\mu_d^2}{d_{0,d} + k_d} s^2 + \frac{2d_{1,d}\mu_d}{d_{0,d} + k_d} s + 1 = 0 \quad (51)$$

This equation can be rewritten in the following form:

$$(\mu_d^0)^2 s^2 + 2d_d^0 \mu_d^0 s + 1 = 0, \quad (52)$$

with

$$\mu_d^0 = \frac{\mu_d}{d_{0,d} + k_d} \sqrt{d_{0,d} + k_d}, \quad (53)$$

and

$$d_d^0 = \frac{d_1}{d_{0,d} + k_d} \sqrt{d_{0,d} + k_d}. \quad (54)$$

The design rules are:

$$\mu_d^0 \leq 0.1\tau_d, \; d_{dmin}^0 \leq d_d^0 \leq d_{dmax}^0 \quad (55)$$

Table 1: Example Motor Parameters

| | | |
|---|---|---|
| $R_s$ | stator resistance | 0.18 $\Omega$ |
| $R_r$ | rotor resistance | 0.15 $\Omega$ |
| $L_s$ | stator inductance | 0.0699 $H$ |
| $L_r$ | rotor inductance | 0.0699 $H$ |
| $M$ | mutual inductance | 0.0680 $H$ |
| $J$ | rotor moment of inertia | 0.0568 $kgm^2$ |
| $n_p$ | number of pole pairs | 1 |
| $T$ | rated power | 15kW |

Table 2: Constants

| $\sigma$ | $\eta$ | $\beta$ | $\mu$ | $\gamma$ |
|---|---|---|---|---|
| 0.0536 | 2.1459 | 259.5 | 8.3 | 85.89 |

# 6 Refined Analysis of Inner Control Loops

In this chapter the inner loops are analyzed in more detail assuming finite values of $\mu$-parameters. The parameters of an example motor given in tables 1 and 2 are used further in this paper.

## 6.1 Analysis of the current controller

Assuming that the flux is constant and using $\psi_d = Mi_d$ the current equation (14) is transformed to:

$$\frac{di_q}{dt} = (-\gamma - \eta)i_q - (\beta M - 1)n_p\omega i_d + \frac{1}{\sigma L_s}u_q \qquad (56)$$

If the drive is accelerating, a slope-wise speed forms an important disturbance in the system. Therefore it is reasonable to set $d_{0,q} = 0$ and $\mu_q = \tau_q$ in the current controller in (44) to have the integral action keeping the control error as small as possible. The current control loop is shown in Figure 2 with $\tau_1 = 1/(\gamma + \eta)$, $d(t) = (\beta M - 1)n_p\omega i_d$ and $B_1 = (\gamma + \eta)^{-1}(\sigma L_s)^{-1}$. The block $B_1^{-1}$ is used to normalize the gain, and is the new input for the controller.
The parameters relevant for the current loop are given in Table 3. The two different time scales in the system are seen in this figure. The filter is the slow time scale, and the control loop the fast time scale.

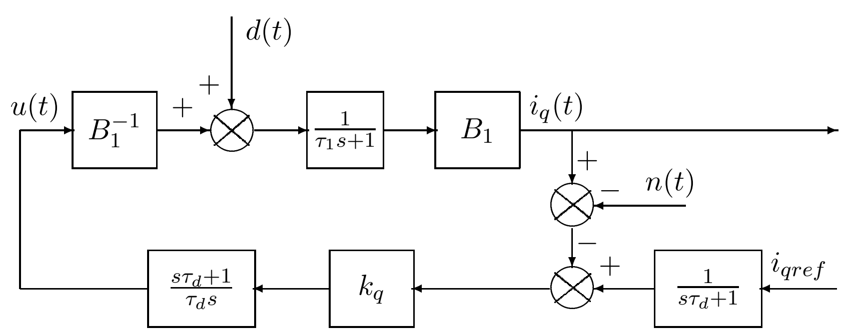


Figure 2: The current control subsystem

Table 3: Current dynamics parameters

| $\gamma$ | $\eta$ | $n_p$ | $\beta$ | $\tau_1$ | $B_1$ |
|---|---|---|---|---|---|
| 85.89 | 2.14 | 1 | 260 | 11.4e-3 | 3.03 |

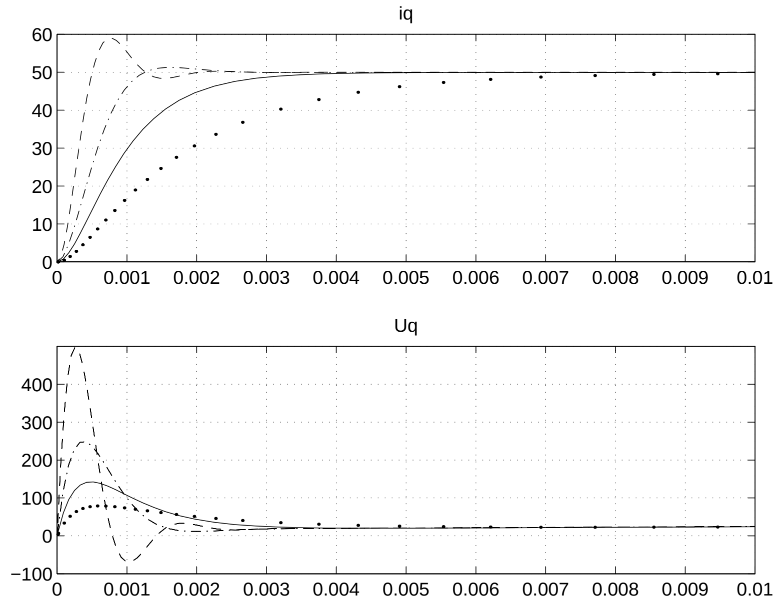


Figure 3: Simulation plot for $k_q$=50 and $\tau_q$ =.2e-3 (dashed), .5e-3 (dash-dot), 1e-3 (solid), 2e-3 (dots).

Assuming zero noise and zero disturbances there is:

$$i_q(s) = k_q \frac{1}{\tau_q s(s\tau_1 + 1) + (s\tau_q + 1)k_q} i_{qref}(s) \tag{57}$$

If $\tau_q = \tau_1$ then

$$i_q(s) = k_q \frac{1}{(s\tau_q + 1)(s\tau_q/k_q + 1)} i_{qref}(s) \tag{58}$$

and the charactristic polynomial of the fast motion subsystem overlaps with that of (51). With large enough gain both (57) and (58) reduce to:

$$i_q(s) = \frac{1}{s\tau_q + 1} i_{qref}(s) \tag{59}$$

which is independent of the plant time constant $\tau_1$.
The gain must be large enough to track the reference trajectory and have a small steady state error. On the other side, when choosing the gain larger the system becomes more sensitive to high frequency noise. As a result, a tradeoff between robustness and sensitivity is to be chosen. More details about designing controllers to operate in the conditions of high-frequency sensor noise can be found in (Błachuta, Yurkevich, and Wojciechowski, 1997). Figure 3 shows the simulation result for different $\tau_q$ and constant $k_q$. From Fig. 4 the influence is shown for choosing different values of $k_q$. For larger $k_q$ the system better follows the trajectory, is more robust against disturbances, and has a smaller steady-state error.

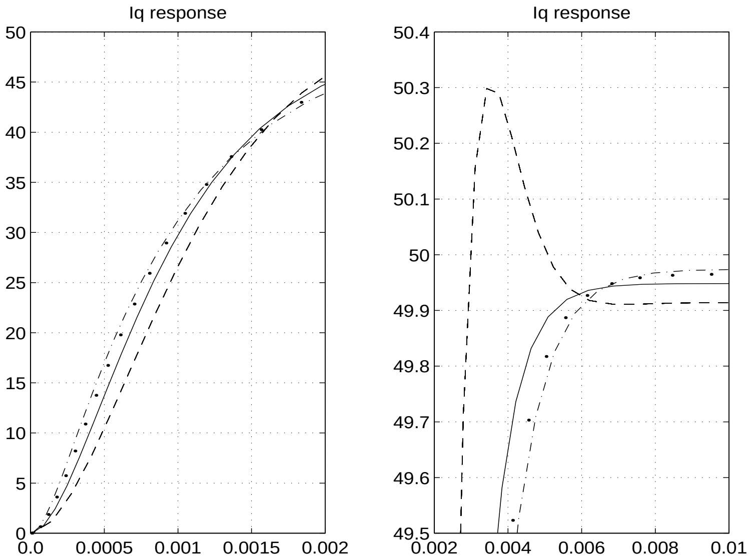


Figure 4: Simulation plot for different $k_q$ and constant $\tau_q$, $\tau_q$=1e-3, $k_q$=30 (dashed), $k_q$=50 (solid), $k_q$=75 (dots), $k_q$=100 (dash-dot).

Table 4: Flux dynamics parameters

| $\eta$ | $\gamma$ | $\beta$ | $\tau_2$ | $\tau_3$ | $B_2$ | $M$ |
|---|---|---|---|---|---|---|
| 2.146 | 85.89 | 259.5 | 11.7e-3 | 476e-3 | 38.92 | 0.068 |

## 6.2 Analysis of the flux controller

With the assumption $d\psi_d/dt = 0$ equation (13) determining $i_d$ simplifies to:

$$\frac{di_d}{dt} = (-\gamma + M\eta\beta)i_d + n_p\omega i_q + \eta\frac{i_q^2}{i_d} + \frac{1}{\sigma L_s}u_d \tag{60}$$

With (13) and $\tau_1 = 1/(\gamma + M\eta\beta)$, $\tau_2 = 1/\eta$ and $B_2 = M/((\gamma - \eta\beta M)\sigma L_s)$ this can be presented as a linear system disturbed by $d(t) = n_p\omega i_q + \eta i_q^2/i_d$. The block $B_2^{-1}$ is used to normalize the gain, and is the new input for the controller. The flux control subsystem is displayed in Fig. 5. In Table 4 the parameters of the flux subsystem are given. The transfer function from reference input to output is defined by:

$$\psi(s) = \frac{k}{\mu_d s(\mu_d s + 2d_{1,d})(\tau_2 s + 1)(\tau_3 s + 1) + (\tau_d^2 s^2 + 2\alpha_d\tau_d s + 1)k}\psi_{dref}(s) \tag{61}$$

The effects of changing parameters can be visualized by root locus plots in Fig. 6.
If the gain is high enough, the poles of the closed loop system are on the asymptote located at

$$\sigma_c = \frac{-2d_{1,d}/\mu_d - \gamma - \eta + \alpha_d/\tau_d}{2} \tag{62}$$

The simplest case is if the controller zeros exactly cancel the two poles of the flux dynamics and then $\sigma_c = -d_{1,d}/\mu_d$. If the poles and zeros are different but co-measurable and $\mu_d$ is small enough the

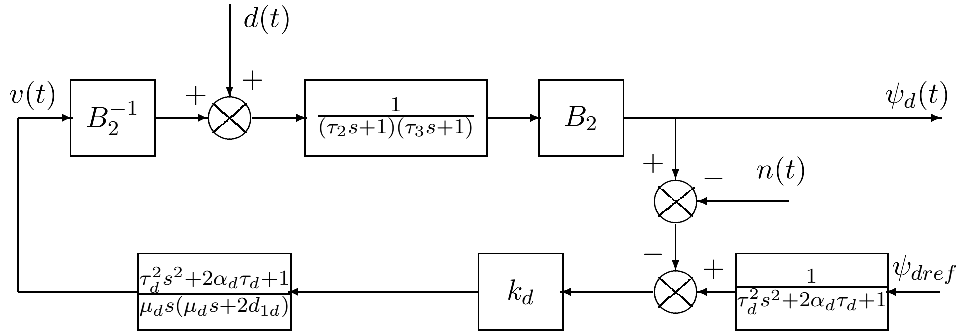


Figure 5: The flux control subsystem

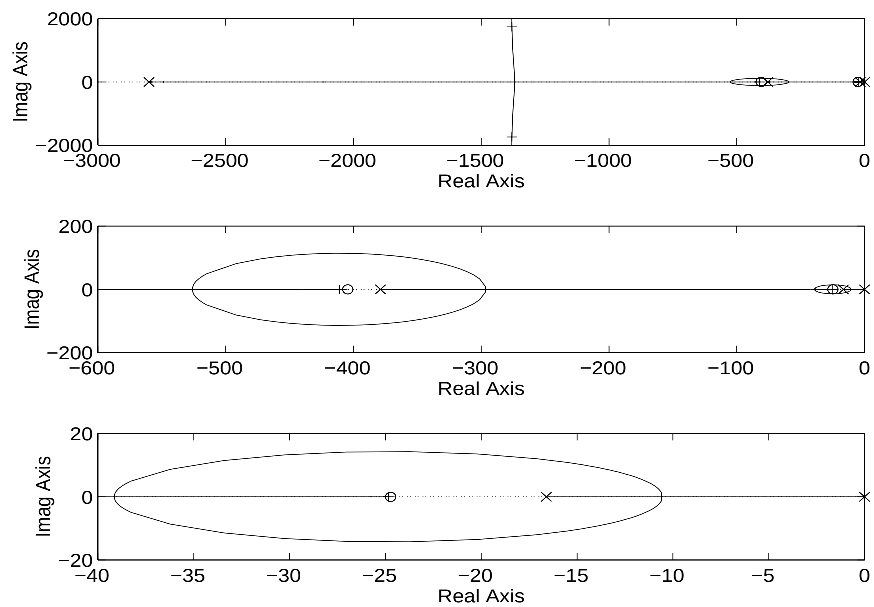


Figure 6: Root locus if controller zeros do not cancel flux poles. The upper picture shows the total view of the root locus, the two other pictures are zoomed views of the upper.

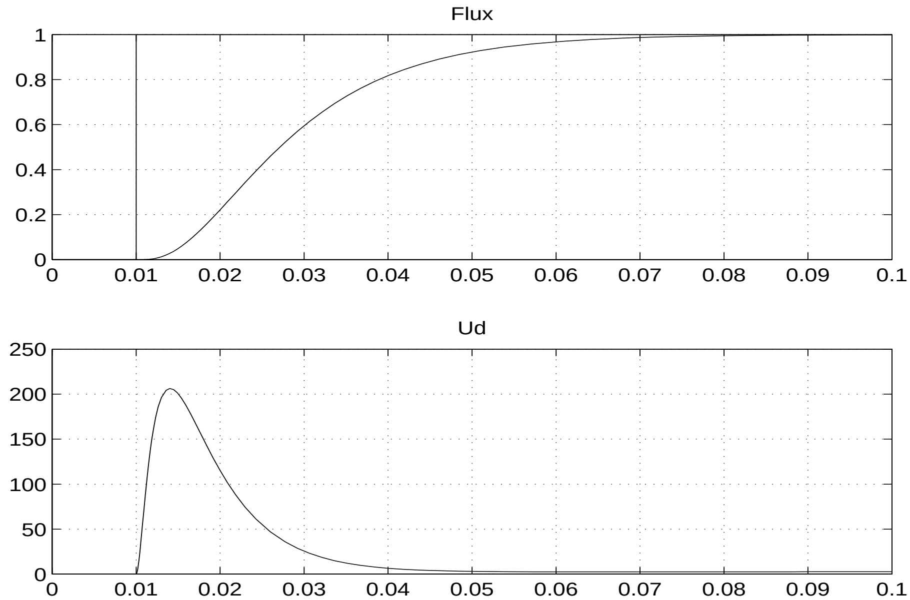


Figure 7: Flux response with the optimized controller, $\omega = 0, \dot{\rho} = 0$

Table 5: DCM controller parameters

| $\alpha_d$ | $\tau_d$ | $d_{0,d}$ | $d_{1,d}$ | $\mu_d$ | $k_d$ |
|---|---|---|---|---|---|
| 1 | 1e-2 | 0 | 1.4 | 0.001 | 1.6 |

situation is similar to the previous case. Figure 7 shows the flux response for the optimized controller. To check the influence of disturbances on the flux control a step is made on $i_q$ with constant flux and zero speed ($t = 0.5$ s). Later the same step is made with speed at a high value ($t = 0.6$ s, and $t = 1.0$ s). The controller parameters are collected in Table 5.

# 7 Time Optimal Position Control

The position control problem in this section refers to a system, whose mechanical equations are given by:

$$\frac{d\theta}{dt} = \omega \tag{63}$$

$$J\frac{d\omega}{dt} = T_e - T_L, \tag{64}$$

with $J$ the moment of inertia, $T_e$ electrical torque, and $T_L$ a constant load torque.

The motor along with the inverter has several electrical, mechanical and thermal limits. For example, electrical constraints are given by:

$$u_a^2 + u_b^2 = u_q^2 + u_d^2 \leq V_{max}^2 \tag{65}$$

$$i_a^2 + i_b^2 = i_q^2 + i_d^2 \leq I_{max}^2, \tag{66}$$

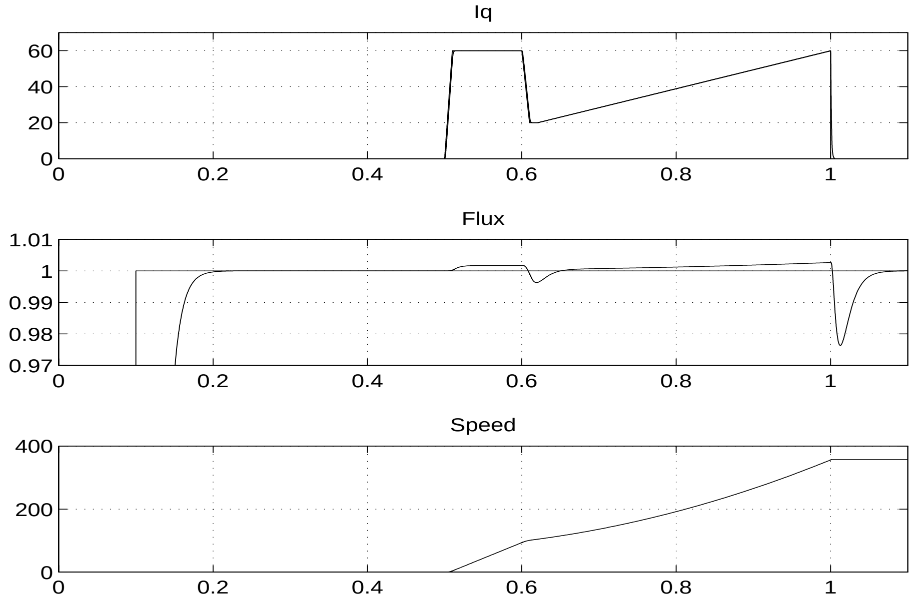


Figure 8: Influence of disturbances on $\psi_d$

where $V_{max}$ and $I_{max}$ are respectively the fixed voltage and current limit, which can be translated to speed and acceleration limits. In (Bodson, Chiasson, and Novotnak, 1994) a flux reference was generated which maximizes the torque at arbitrary speed without violating the voltage and current limits (Bodson, Chiasson, and Novotnak, 1995). Unfortunately the analysis in (Bodson *et al.*, 1995) was performed assuming steady-state values which is only useful when electrical transients are much faster than the mechanical ones. This only applies for micro-motors and is useless for larger motors. Therefore in our setup the flux is kept constant and a maximum speed limit is imposed.

For given bounds on current and velocity the position control problem can be stated as a time optimal control problem. Under assumption that the current loop is fast the system can be approximated by a double integrator system of equations (63)-(64) with $T_e$ being a control variable for which the time optimal solution consists of two intervals of maximum acceleration/deceleration. If the position error is large enough there is a third interval with maximum speed and zero acceleration. The solution to the problem with an extra time constant $\tau_q$, (Ryan, 1982), is difficult to be found and implement.

The relation between position and velocity during deceleration is as follows:

$$\omega = \begin{cases} \sqrt{2a_{max}|\Delta\theta|}\,\mathrm{sign}\,(\Delta\theta), & |\omega| < \omega_{max} \\ \omega_{max}\,\mathrm{sign}\,(\Delta\theta), & |\omega| \geq \omega_{max} \end{cases} \tag{67}$$

with $\Delta\theta = \theta_{ref} - \theta$. If the load torque $T_L$ is known $a_{max}$ can be calculated from Eq. (11). The function in (67) can be implemented as a nonlinear block directly in the control loop of Fig. 1 or it can be used to control the model (63)-(64), which generates feed-forward signals for a linear cascaded control system (Leonhard, 1990).

In the former case, to work with the non-ideal system having the additional time constant $\tau_q$, the speed controller is a high-gain linear controller whose output saturates at $|i_{qref}| = i_{qmax}$ rather than a relay, and to avoid infinite gain the function in (67) is linearized around the origin. In Fig. 9 the nonlinear function is shown. The solid line is the ideal function, and the dashed line the linearized one. In Table 6 the simulation parameters are collected.

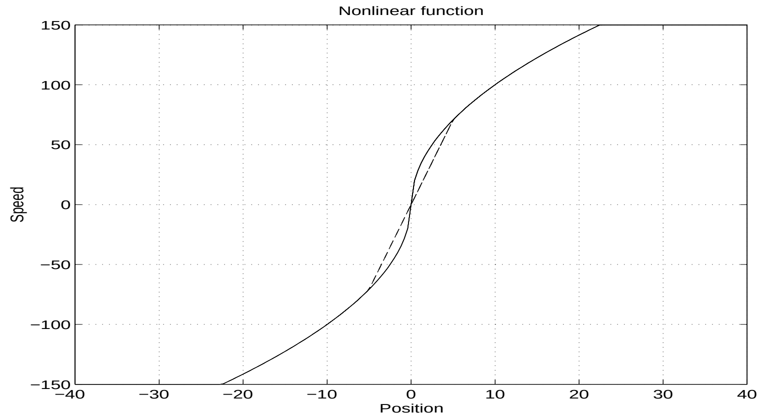


Figure 9: The nonlinear function with a linear zone

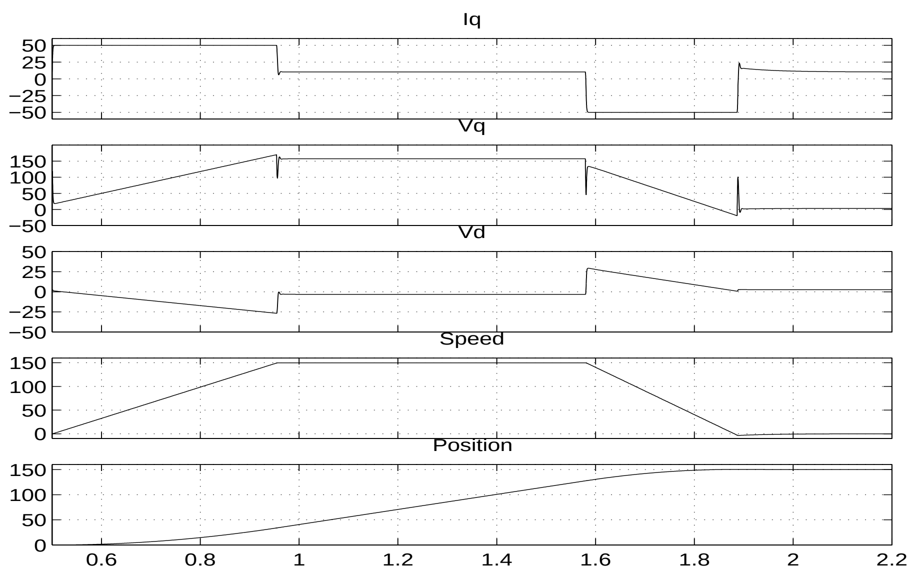


Figure 10: Large initial position error with $k_{speed}$=80

# 8 Concluding Remarks

The inner loops are controlled by Dynamic Contraction Method controllers which have advantages above PI controllers. A comparison between PI and DCM was done in (van Duijnhoven, 1998) if the input was stepwise. In this case the DCM controller was superior. In PI case the gain could not be as high as in the DCM case, because this resulted in over-steered stator voltages. Due to the high gain the DCM controller is less sensitive to disturbances and has a smaller steady state error.

In (van Duijnhoven, 1998) two control structures which base on the two integrator problem were examined. The non-feed-forward structure was superior if torque was not known. If small initial position errors appear the feed-forward structure is preferred. In case of large position errors and unknown but estimated torque the non-feed-forward structure is better.

In (van Duijnhoven, 1998) observers (Novotnak, Bodson, and Chiasson, 1995) were added to the motor control structure. They worked well if there was a good observation of the flux angle. Unfortunately, when the rotor resistance varied the flux angle was not observed correctly. A solution to robustify the control system is to construct an observer for the rotor resistance (Gorter, 1997).

Table 6: Simulation parameters for non-linear structure

| $i_{max}$ | $\omega_{max}$ | $T_L$ | $J$ | $k_{speed}$ | $\tau_q$ | $k_q$ | linear zone |
|---|---|---|---|---|---|---|---|
| 50 A | 150 rad/s | 10 Nm | 2*0.0586 | 80 | 1e-3 | 50 | 5 |

## References


Bartolini, G., P. Pisu, M. Marchesoni, and E. Usai (1998). "Chattering reduction and robust position control in induction motor with second-order VSS," *Int. Journal of System Science*, **29**, pp. 11–12.

Błachuta, M., V. Yurkevich, and K. Wojciechowski (1997). "Robust quasi NID aircraft 3D flight control under sensor noise," in *CD-ROM Proceedings of the 5th IEEE Mediterranean Conference on Control and Systems*, IEEE CSS, Paphos, Cyprus. Accepted for publication in *Kybernetika*.

Blaschke, F. (1971). "Das Prinzip der Feldorientierung, die Grundlage für die TRANSVEKTOR-Regelung von Drehfeldmaschinen," *Siemens-Zeitschrift*, **45**, pp. 757–760.

Bodson, M., J. Chiasson, and R. Novotnak (1994). "High-performance induction motor control via input-output linearization," *IEEE Control Systems Magazine*, **14**, pp. 25–33.

Bodson, M., J. Chiasson, and R. Novotnak (1995). "A systematic approach to selecting flux references for torque maximization in induction motors," *IEEE Trans. Control Systems Technology*, **3**, pp. 388–397.

Gorter, R. (1997). *Grey-box identification of induction machines*, Ph.D. thesis, Eindhoven Technical University.

Krause, P. and C. Thomas (1965). "Simulation of symetrical induction machinery," *IEEE Trans. Power Apparatus Syst.*, **84**, pp. 1038–1053.

Leonhard, W. (1990). *Control of Electrical Drives*, Springer-Verlag. Second edition.

Marino, R., S. Peresada, and P. Valigi (1993). "Adaptive input-output linearizing control of induction motors," *IEEE Trans. Automatic Control*, **38**, pp. 208–221.

Novotnak, R., M. Bodson, and J. Chiasson (1995). "Nonlinear speed observer for high-performance induction motor control," *IEEE Trans. Industry Applications*, **42**, pp. 337–343.

Ryan, E. (1982). *Optimal relay and saturating control system synthesis*, Peter Peregrinus.

van Duijnhoven, M. (1998). *Time optimal position control of an induction motor based on the Dynamic Contraction Method*, Master's thesis, Eindhoven Technical University. Written under supervision of M.J. Błachuta.

Yurkevich, V. (1995a). "Decoupling of uncertain continuous systems: Dynamic Contraction Method," in *Proc. of the 34th Conference on Decision & Control*, IEEE CSS, New Orleans, pp. 196–201.

Yurkevich, V. (1995b). "A new approach to design of control systems under uncertainty: Dynamic Contraction Method," in *Preprints of the 3-rd IFAC Symposium on Nonlinear Control Systems Design*, IFAC, Tahoe City, vol. 2, pp. 443–448.